Applied Catalysis B: Environmental 94 (2010) 117–124

Contents lists available at ScienceDirect

Applied Catalysis B: Environmental

journal homepage: www.elsevier.com/locate/apcatb

Supported gold catalysts for the decomposition of VOC: Total oxidation of propene in low concentration as model reaction

Laurent Delannoy *, Katia Fajerwerg [1], Pandian Lakshmanan, Claude Potvin, Christophe Méthivier, Catherine Louis

Laboratoire de Réactivité de Surface, UMR 7197 CNRS, Université Pierre et Marie Curie-UMPC, 4 place Jussieu, 75252 Paris Cedex 05, France

ARTICLE INFO

Article history:
Received 10 September 2009
Received in revised form 28 October 2009
Accepted 29 October 2009
Available online 4 November 2009

Keywords:
Gold catalysts
Ceria
Titania
Alumina
Total oxidation
VOC decomposition
Propene oxidation
CO oxidation
Gold oxidation state
Deposition–precipitation with urea
DRIFTS
XPS

ABSTRACT

Supported gold catalysts prepared by deposition–precipitation with urea were studied in the reaction of oxidation of propene in low concentration in a large excess of oxygen, so as to mimic the conditions of catalytic decomposition of a volatile organic compound of hydrocarbon-type (1200 ppm C_3H_6, 9% O_2 in He). Several parameters were investigated: the nature of the oxide support (alumina, titania, ceria), the gold loading, the conditions of catalyst activation (oxygen or hydrogen). Titania and alumina alone did not show any conversion in C_3H_6 oxidation up to 500 °C, but when gold was added (1 wt%), active catalysts were obtained with a higher activity for titania than for alumina. Ceria was the only support showing activity, and gold on ceria (1 wt%) led to the most active catalyst. For the Au/CeO_2 system, activation under H_2 at 300 °C leads to more active catalysts than activation in O_2/He at 500 °C, especially for gold loadings lower than 1 wt%. XPS and CO oxidation performed at RT showed that gold on CeO_2 was fully reduced to Au^0 after activation under H_2 whatever the gold loading. In contrast, after calcination, most of the gold remained under the initial Au^{III} state for the low loaded samples ($\leq$1 wt%) whereas part of it was reduced for the 4 wt% Au/CeO_2. Thus, ceria seems to be able to stabilise gold as Au^{III} up to a limited loading. Change in the gold oxidation state was detected for the calcined Au/CeO_2 (1 wt%) during C_3H_6 oxidation performed at increasing temperature, using CO oxidation and DRIFTS combined to CO adsorption. Indeed, gold, initially Au^{III}, starts reducing at 100 °C to form metallic gold Au^0, which was the active species for the reaction. Above 300 °C, when 100% conversion was achieved, reoxidation of metallic gold species was observed.

1. Introduction

Emission into the atmosphere of volatile organic compounds (VOC, more than 1500 different molecules including aromatic solvents, hydrocarbons, oxygenated compounds and chlorocarbons) arising from domestic or industrial activities leads to pollution that is harmful to public health; pollution may be caused directly by those compounds or by others formed in the atmosphere by chemical reactions brought about by sunlight or ozone.

Gas streams requiring treatment often contain only low concentrations of pollutant (100–2000 ppm), and catalytic combustion is a promising technology for the destruction of VOCs. Supported noble metals (Pt, Pd, Rh) on the one hand and transition metal oxides such as cobalt, chromium, or manganese oxides on the other hand are the two categories of catalysts active for the VOCs decomposition. Gold-based catalysts, which have been more recently investigated, are also promising for this type of issue. Au/Fe_2O_3 [1–3], Au/Al_2O_3 [4,5] and Au/CeO_2 [6–9] have been found to have high activities for the decomposition of different kind of VOCs. The catalytic properties of gold catalysts in these oxidation reactions have been notably explained by the capacity of small gold particles to increase the mobility of the lattice oxygen in the case of gold supported on ferric oxide [2,3], and, for Au/CeO_2, to the weakening of the surface Ce–O bonds adjacent to gold atoms, leading to the activation of the surface capping oxygen [8] which would be involved in a Mars–van Krevelen type reaction mechanism [2,3,8,9]. Regarding the removal of hydrocarbon-type VOCs, gold catalysts have been used for the oxidation of various saturated and unsaturated hydrocarbons [10–16]; Au/Co_3O_4 exhibits the highest catalytic activity, perhaps because the support itself is also very active [10,16,17]. Based on the temperature at which 50% conversion ($T_{50\%}$) was reached for the oxidation of propane and propene, the activity for 10 wt% Au catalysts decreased in the following order: $Au/Co_3O_4 > Au/NiFe_2O_4 > Au/ZnFe_2O_4 > Au/Fe_2O_3$ [18].

* Corresponding author.
E-mail address: laurent.delannoy@upmc.fr (L. Delannoy).
[1] Present address: Laboratoire de Chimie de Coordination, UPR 8241 CNRS, 205 Route de Narbonne, 31077 Toulouse Cedex 4, France.

0926-3373/$ – see front matter © 2009 Elsevier B.V. All rights reserved.
doi:10.1016/j.apcatb.2009.10.028

The aim of the study was to explore the properties of gold catalysts in the reaction of oxidation of propene in low concentration in a large excess of oxygen, so as to mimic the conditions of catalytic decomposition of a volatile organic compound of hydrocarbon-type. Parameters directly related to the nature of the catalysts (nature of the support, gold loading and activation conditions) were investigated. We also focused on the influence of the oxidation state of gold on the catalytic activity. Indeed, in a former paper [19], it was shown that, under our reaction conditions, only metallic gold Au^0 supported on reducible supports such as TiO_2 or CeO_2 was active in the reaction of CO oxidation at room temperature, and that Au^{III} species was inactive. We also observed that, in some cases, the oxidation state of gold changed during the CO oxidation reaction, from an inactive oxidised state towards an active metallic state. Thus, we examined the possible modifications of the gold oxidation state during the propene oxidation reaction. For that purpose, the CO oxidation reaction was used as a tool for the characterisation of the oxidation state of gold on various supports.

2. Experimental

2.1. Catalyst preparation

The catalysts were prepared by deposition–precipitation with urea (DPU) as described previously [20,21] using Titania (P25, Degussa, 50 $m^2\,g^{-1}$, 70% Anatase, 30% Rutile), ceria (HSA5, Rhodia, 200 $m^2\,g^{-1}$, pre-calcined under air at 500 °C), and alumina (AluC Degussa, 110 $m^2\,g^{-1}$, δ-type) were used as supports. For each preparation, 3 g of support and 60 mg of $HAuCl_4{\cdot}3H_2O$ (Acros Chemicals) were used, in order to achieve a nominal gold loading of 1 wt%. According to a former study [19], such type of preparation allows to obtain samples containing the same expected gold loading of 1 wt%, and chlorine content always below the detection limit of measurement (<200 ppm).

A 300 mL solution containing $HAuCl_4$ (5×10^{-4} M), 0.9 g of urea ([urea] ~ 100 [Au]) and the support (3 g) was prepared, stirred at 80 °C for 16 h in a dark and closed reactor. The solid was separated by centrifugation, washed four times with distilled water (with centrifugation between each washing). After the third washing, a few drops of silver nitrate (0.1 M) were added to the washing solution, and did not show any AgCl precipitation. The samples were then dried under vacuum at RT for 12 h, resulting in "*as-prepared*" samples. Other gold amounts (0.02, 0.5 and 4 wt%) were also loaded on ceria according to the same preparation procedure. After drying, the samples were stored at RT under vacuum in a desiccator, away from light in order to prevent any uncontrolled reduction of gold [22]. The colour of the *as prepared* catalysts depended on the nature of the support, salmon-orange with alumina, yellow with ceria (same colour as the pure ceria support) and white for titania.

Before characterisation, the gold catalysts were thermally treated, either under H_2 (100 mL min^{-1}) from RT to 300 °C (2 °C min^{-1}) with a 2 h plateau at 300 °C, or under O_2 (9% in He) (150 mL min^{-1}) from RT to 500 °C (2 °C min^{-1}) with a 2 h plateau at 500 °C. Note that for the sake of brevity, these treatments are called reduction and calcination, respectively, in the following, but this does not presume the gold oxidation state in the samples.

2.2. Techniques of characterisation

Chemical analyses of Au, Cl and metal cation of the support were performed by inductively coupled plasma atom emission spectroscopy (ICP/AES) at the CNRS Centre of Chemical Analysis (Vernaison, France). The Au weight loading of the samples was expressed in gram of Au per gram of sample: Au (wt%) = $[m_{Au}/(m_{Au} + m_{support})] \times 100$.

TEM analysis was performed using a JEOL JEM-100 CX II microscope operating at 100 kV equipped with a TCD camera (keen view). Gold particle size measurement was performed using ITEM software on digitised micrographs. Note that the particles were measured one by one and not automatically. The limit of size detection was about 1 nm, but it was easier to measure gold particles on titania than on alumina. Moreover, it was not possible to measure them on ceria because of the too low contrast between ceria and gold particles due to the high atomic number of Ce and the high specific surface area of ceria [23]. The average metal particle sizes d_{Au} were determined from the measurement of at least 300 particles, and d_{Au} was calculated using the following formula: $d_{Au} = \Sigma n_i d_i / \Sigma n_i$ (arithmetic mean), where n_i is the number of particles of diameter d_i.

The XRD patterns were recorded on a Siemens diffractometer (D500) using the Cu Kα radiation. XPS spectra were collected on a SPECS (Phoibos MCD 150) X-ray photoelectron spectrometer, using a Mg Kα ($h\nu$ = 1253.6 eV) X-ray source. After collection, the binding energies were calibrated with respect to either the C–C/C–H components of the C 1s peak at a binding energy of 284.8 eV [24] or the Ce^{4+} $3d_{3/2}$ peak at the binding energy of 916.9 eV [25]. The atomic ratio calculations were performed after normalisation using Scofield factors [26]. All spectra processing were carried out using the Casa XPS software package.

Infrared spectroscopy was performed with an IFS66V Bruker spectrometer using a DRIFTS cell (collector from Spectratech) and a MCT detector.

2.3. Catalytic reaction

The reaction of propene oxidation was carried out with 150 mg of catalyst in a gradientless flow microreactor in pyrex (8 mm of internal diameter). The catalysts were activated *in situ*, in H_2 at 300 °C or O_2/He at 500 °C, according to the same procedure described above. Then, the catalysts were cooled to 50 °C under He or O_2/He, respectively, and the reaction mixture consisting of 1200 ppm C_3H_6 and 9% O_2 in He was introduced with a flow rate of 150 mL min^{-1}, which corresponds to a GHSV of 72 000 h^{-1}. The catalysts were heated under this gas mixture at a rate of 2 °C min^{-1} up to 300 or 500 °C, depending on the activation treatment. Every 25 or 50 °C, temperature was kept constant for about 45 min during which several analyses were performed with a gas chromatographer (Perichrom 2100, FID detector) using a capillary fused silica column (0.32 mm, 50 m) with a coating CP-WAX 57 CB. Conversion was calculated with respect to the peak area of propene measured at the outlet of the reactor. CO_2 formation was monitored using an infrared detector (ADC). To detect other possible compounds, i.e., allylic alcohol or acrolein for instance, mass spectrometer (Hiden Quadrupole HPR20) was used in some experiments with catalyst mass 50 mg instead of 150 mg. Several tests of repeatability and reproducibility were performed to validate the results obtained.

CO oxidation was performed with a flow-type packed-bed microreactor at room temperature and atmospheric pressure with a feed of 1% CO and 9% O_2 in He (total flow rate 230 mL min^{-1}, GHSV = 330 000 h^{-1}). The reaction was performed after *in situ* activation of the gold catalysts (50 mg) with O_2 in He at 500 °C or H_2 at 300 °C. Then the reactor was flushed with He at RT (in a water bath), and replaced by the reaction mixture. The CO consumption and CO_2 production were monitored with a Maihak Gas IR Analyzer S710.

In order to evaluate possible changes of gold oxidation state during propene oxidation, a 1 wt% Au/CeO_2 sample calcined at 500 °C was submitted to propene oxidation (1200 ppm C_3H_6/9% O_2/He; 230 mL min^{-1}, GHSV ~165 000 h^{-1}) from RT to 500 °C. The measurement of propene conversion was performed in isothermal

conditions by stepwise increase of the temperature as mentioned above. After each temperature in propene oxidation, the catalyst was cooled down to RT under He, then the activity in CO oxidation (1% CO/9% O_2/He; 230 mL min^{-1}, GHSV ~165 000 h^{-1}, T = 20 °C) was measured at RT. Afterwards, the catalysts were heated up to the next temperature under He then exposed to the reaction mixture of propene oxidation. The same type of experiment was performed directly in the DRIFT cell, with 40–50 mg of *as-prepared* samples. The 1 wt% Au/CeO_2 catalyst was calcined at 500 °C in situ in the DRIFT cell. After propene oxidation reaction (1200 ppm C_3H_6/9% O_2/He (50 mL min^{-1}) in the DRIFT cell at temperature between 100 and 500 °C for 20 min) and cooling down the sample at RT, the cell was purged with He before introduction of 1% CO/He (50 mL min^{-1}) at room temperature for 10 min. The spectrum recorded in He was used as reference and the intensity of the spectrum in CO/He atmosphere was expressed as $\log(I_{ref}/I_{CO})$.

3. Results and discussion

3.1. Influence of the nature of support

For this first set of experiments, the samples (50 mg) were calcined *in situ* in 9% O_2/He at 500 °C and a mass spectrometer was used to detect possible by-products arising from partial oxidation of propene, i.e., allylic alcohol, acrolein.

Fig. 1 reports the conversion of propene as a function of temperature for the gold samples (1 wt% Au) supported on titania, alumina and ceria, and for the corresponding oxide supports activated in the same way. Ceria is the only support which shows activity. Titania and alumina alone do not show any conversion up to 500 °C. When gold is supported on alumina and titania, the catalysts are active, with a higher activity for gold on titania than on alumina. Gold on ceria is the most active catalyst. The addition of gold to ceria leads to a decrease of the $T_{50\%}$ (temperature at which 50% conversion of propene is reached) by around 100 °C with respect to ceria alone.

Apart from CO_2, mass spectrometer analysis reveals the presence of only traces of allylic alcohol and/or acrolein at the outlet of the reactor. This indicates that the selectivity to CO_2 is close to 100% and that oxidation of propene is quasi-total for all the catalysts.

3.2. Influence of the gold loading

Since gold on ceria exhibits the best catalytic performance, the influence of the gold loading (0.02, 0.5, 1 and 4 wt%) was investigated on this support. The catalysts (150 mg) were activated *in situ* in 9% O_2/He at 500 °C. Fig. 2 shows that the curves shift towards lower temperatures as the gold loading increases, indicating, as expected, increasing activity with the gold loading. It is worth noting that the temperature shift, with respect to pure ceria, is significant even for a gold loading as low as 0.02 wt%.

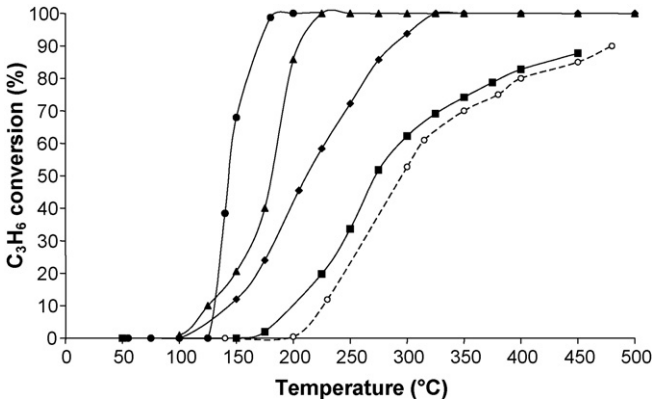

Fig. 2. Propene conversion versus temperature over ceria-based samples activated under O_2/He at 500 °C: CeO_2 (○), 0.02% Au/CeO_2 (■), 0.5% Au/CeO_2 (◆), 1% Au/CeO_2 (▲), 4% Au/CeO_2 (●).

3.3. Influence of the activation treatment

Au/CeO_2 catalysts (0.02, 1 and 4 wt%) were also activated under H_2 (reduction) at 300 °C. The comparison of the propene conversion for the Au/CeO_2 samples activated under O_2/He (calcination) at 500 °C and reduction at 300 °C is reported in Fig. 3. It shows that the samples with the lowest gold loadings (0.02 and 1 wt%) are more active after activation under reduction than after calcination, this is more clearly visible for the 0.02 wt% sample than for the 1 wt% sample. The 4 wt% Au/CeO_2 catalyst exhibits exactly the same catalytic behaviour whether it was calcined or reduced before reaction; the two curves are perfectly superimposed.

3.4. Characterisation of the samples after activation treatments and discussion

The samples containing 1 wt% gold supported on titania, alumina and ceria have been already characterised in a former paper [19], and the results are reported in Table 1. It is well-known that Au^{III} species is unstable on temperature, thus, whenever

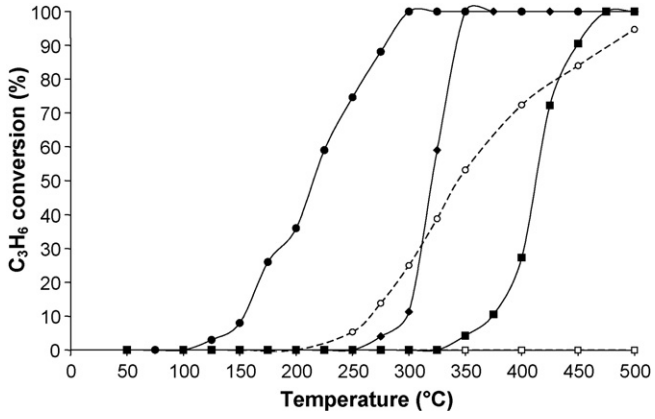

Fig. 1. Propene conversion versus temperature over samples activated under O_2/He at 500 °C: TiO_2 (◇), Al_2O_3 (□), CeO_2 (○), 1%Au/TiO_2 (◆), 1%Au/Al_2O_3 (■) and 1%Au/CeO_2 (●).

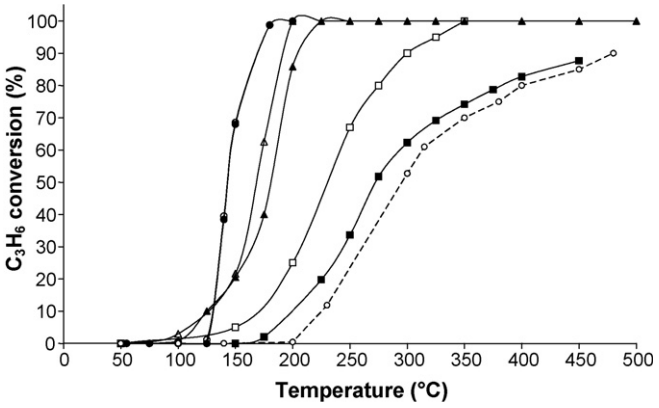

Fig. 3. Propene conversion versus temperature over Au/CeO_2 activated under O_2/He at 500 °C or H_2 at 300 °C: CeO_2 O_2 (○; dotted line), 0.02% Au/CeO_2 O_2 (■), 0.02% Au/CeO_2 H_2 (□), 1% Au/CeO_2 O_2 (▲), 1% Au/CeO_2 H_2 (Δ), 4% Au/CeO_2 O_2 (●), 4% Au/CeO_2 H_2 (○).

Table 1
Characterisation of gold on titania, alumina, and ceria after activation treatments either under oxygen or hydrogen and catalytic properties in CO oxidation and propene oxidation.

Sample	Gold loading (wt%)	Activation treatment	Colour	Oxidation state		TEM	CO oxidation (at RT)	$T_{50\%}$ propene oxidation (°C)	
				EXAFS [a]	XPS	Gold particle size (nm)	Activity[c] ($mmol_{CO}\,s^{-1}\,g_{Au}^{-1}$)	Catalyst mass (50 mg)	Catalyst mass (150 mg)
1 wt% Au/TiO_2	1.1	H_2/300 °C	Purple	Au^0	–	1.7	1.08[a]	–	–
		O_2/500 °C	Purple	Au^0	–	3.9	0.83[a]	320	–
1 wt% Au/Al_2O_3	0.96	H_2/300 °C	Purple red	Au^0	–	1.9	0[a]	–	–
		O_2/500 °C	Purple red	Au^0	–	3.3	0[a]	410	–
1 wt% Au/CeO_2	1.0	H_2/300 °C	Brown	Au^0	Au^0	<5[b]	0.99[a]	–	165
		O_2/500 °C	Yellow	Au^{III}	Au^{III}, $Au^{\delta+}$, Au^0	–	0[a]	215	180
4 wt% Au/CeO_2	3.9	H_2/300 °C	Dark purple	–	Au^0	<5[b]	0.68	–	140
		O_2/500 °C	Dark purple	–	Au^{III}, $Au^{\delta+}$, Au^0	–	0.54	–	140
0.5 wt% Au/CeO_2	0.55	H_2/300 °C	Brown	–	–	–	0.81	–	200
		O_2/500 °C	Yellow	–	–	–	0	–	215
0.02 wt% Au/CeO_2	0.025	H_2/300 °C	Light brown	–	–	–	–	–	230
		O_2/500 °C	Yellow	–	–	–	–	–	275
CeO_2		O_2/500 °C	Yellow	–	–	–	–	340	290

[a] From ref. [19].
[b] Estimation of the particle size by XRD (no contrast between gold and ceria in TEM).
[c] After 2 min of reaction.

as-prepared gold catalysts are submitted to a thermal treatment under oxidising or reducing atmosphere, gold decomposes and forms metallic particles. This is true for all the oxide supports we have used up to now, except for cerium oxide. In the latter case, combined results of X-ray absorption spectroscopy, CO oxidation reaction and also the sample colour (which remains yellow as for pure ceria) revealed that 1 wt% gold supported on the high specific surface ceria HSA5 was not reduced during calcination at 500 °C and remained in the oxidation state III (Table 1). To our knowledge, ceria, especially with high specific surface area, is the unique support which seems to be able to prevent extensive reduction of Au^{III} species under oxidative treatment. This fact has also been observed by several other authors. Corma and co-workers [27,28] showed that nanocrystalline CeO_2 was able to stabilise Au^{III} on its surface under CO oxidation conditions (with stoichiometric CO and O_2 proportion) but the stability of Au^{III} during thermal activation was not addressed. Vindigni et al. [29] reported that the FTIR spectrum of gold (3 wt%) supported on a mixed oxide CeO_2–TiO_2 and calcined at 400 °C exhibited several CO bands after CO adsorption at RT; the main one at 2166 cm^{-1} was attributed to small cationic clusters. When the sample was then treated in H_2 at 200 °C, this band totally disappeared. Behm and co-workers [30,31] also reported the incomplete reduction of gold (2.7 wt%) supported on CeO_2 (190 $m^2\,g^{-1}$) with 25% of Au^{III} after calcination at 400 °C, according to XPS. They also noticed that 10% of Au was still unreduced after reduction in 10% H_2/N_2 at 400 °C that they attributed to the fact that gold cations may diffuse into the ceria support during thermal treatment, as already proposed by Fu et al. [32]. In another work, Behm et al. observed that gold reducibility depended on the specific surface area of ceria for the same gold loading (2.7 wt%); decreasing ceria surface areas from 285 to 25 $m^2\,g^{-1}$ by calcination treatment from 250 to 900 °C before gold deposition led to an increasing fraction of metallic gold from 75 to 95% after treatment at 200 °C [23]. Deng et al. found by XAFS and XPS that after calcination at 400 °C, no Au^0 was formed in a $Au/Ce(La)O_x$ sample containing 0.5 wt% Au [33].

Our former XAFS study [19] showed that gold on ceria, alumina, titania (1 wt% Au) prepared by DPU was fully reduced into metallic gold after reduction under H_2 at 300 °C, with no detectable traces of Au^{III} or Au^I. The change of colour of the samples to purple, purple red or deep violet, respectively, is also a qualitative indication that at least part of gold is reduced. One can especially note the brown colour of the Au/CeO_2 sample after reduction (Table 1). After reduction under H_2 at 300 °C, the samples contain very small gold particles with almost the same size (~2 nm) on TiO_2 and Al_2O_3 (Table 1). They are slightly larger on alumina and titania when the samples have been calcined in O_2/He (Table 1), in agreement with previous work [34]. As mentioned in Section 2.2, gold particle size on ceria cannot be measured by TEM because of the too low contrast between ceria and gold particles due to the high atomic number of Ce and the high specific surface area of ceria [23]. However, no diffraction line of metal gold was either observed by XRD, indicating that the size of the gold nanoparticles is below 5 nm. Moreover, according to a former XAFS study performed on a similar DPU Au/CeO_2 sample (1 wt%), the extent of the contraction of the Au–Au bond length and the low Au–Au coordination number indicated that the average gold particle size was less than 3 nm [35]. However, since on alumina [36] or titania [20], the gold particle size does not significantly vary when the gold loading increases, we can speculate that this is also true for ceria. We can therefore anticipate that the gold particles are as small on ceria as on titania or alumina.

The series of gold on ceria samples with different loadings have been characterised by XPS and CO oxidation. Table 2 reports the detailed results of XPS characterisation for the samples with 1 and 4 wt% Au. The 0.02 wt% sample has a too low gold loading for XPS detection.

After reduction, gold is fully metallic according to XPS (Table 2 and Fig. 4). Again, the gold particles are not detected by TEM or XRD, and the reduced Au/CeO_2 catalysts are active in CO oxidation.

After calcination, only the sample containing 4 wt% Au has a colour (dark purple) different from the yellow colour of ceria, indicating that part of the gold has been reduced (Table 1). The XPS characterisation (Table 2 and Fig. 4) confirms this result. Regarding the attribution of the XPS Au($4f_{7/2}$) contributions in Table 2, it is fully accepted in the literature that the peak with a binding energy of 84 eV is related to metallic Au^0 and that the peak with a binding energy around 86 eV is due to Au^{III} [30,32,37–41]. Regarding the peak at 84.6 eV, some authors attributed it to Au^I [32,40,42,43], but

Table 2
Binding energy and relative surface area of the Au($4f_{7/2}$) XPS peaks of Au/CeO_2 after various pre-treatments.

Gold loading (wt%)	Treatment	XPS recording temperature	Au°		$Au^{\delta+}$		Au^{3+}	
			BE (eV)	%	BE (eV)	%	BE (eV)	%
1	*As-prepared*	100 K	83.9	17	84.9	46	86.7	37
	O_2/500 °C	100 K	83.6	19	84.8	50	86.7	31
	H_2/300 °C	RT	83.6	100		0		0
4	*As-prepared*	100 K	83.9	6	84.9	47	86.9	47
	O_2/500 °C	100 K	83.9	43	85.0	42	86.6	15
	H_2/300 °C	RT	83.7	100		0		0

other assigned it to small metal clusters as BE shifts of 0.5–1.1 eV relative to bulk Au^0 were obtained as initial [44–46] or final [30,47,48] effects in small Au clusters. For this reason, this peak is noted $Au^{\delta+}$ in Table 2 and we will consider the Au^0 and $Au^{\delta+}$ contributions as reduced species, by comparison with the initial Au^{III} species. It must be noted that during XPS measurement or evacuation in UHV, gold is partially reduced even when the sample is maintained at temperature close to that of liquid nitrogen (100 K). This is clearly observed for the 1 wt% Au/CeO_2 sample, which exhibits the same percentage of reduced species (Au^0 and $Au^{\delta+}$) around 65% whether the sample is *as-prepared* or calcined, i.e., initially contains Au^{III} before XPS measurement. The *as-prepared* 4 wt% Au/CeO_2 sample exhibits a smaller percentage of reduced gold species (53% with 6% of Au^0) whereas after calcination, it is much higher, 85%, indicating that a large part of the gold has been reduced to metallic state during calcination treatment. The reaction of CO oxidation confirms this result since this sample is active at room temperature (Table 1). Thus, it appears from these results that high specific surface ceria is able to stabilise gold in a high oxidation state during calcination at 500 °C up to a limited gold loading of about 1 wt%.

Fig. 1 shows that metallic gold particles are active for the reaction of propene oxidation since metallic gold particles present on alumina and titania supports are active whereas the supports alone are inactive. The fact that gold is more active on titania than on alumina, also indicates a support effect since the gold particle size is roughly the same in the two samples (Table 1). However, the effect of support is not as drastic as in the case of the reaction of CO oxidation at RT. Gold supported on CeO_2 is the most active system and complete oxidation of propene can be achieve with 100% selectivity in CO_2 at temperature below 200 °C in our reaction conditions (Figs. 2 and 3). The redox properties of ceria are probably at the origin of the high activity of the Au/CeO_2 samples. It could notably supply active oxygen species for the oxidation of the hydrocarbons via a Mars and van Krevelen mechanism [4,5,49–51]. Moreover, the presence of gold is known to enhance the

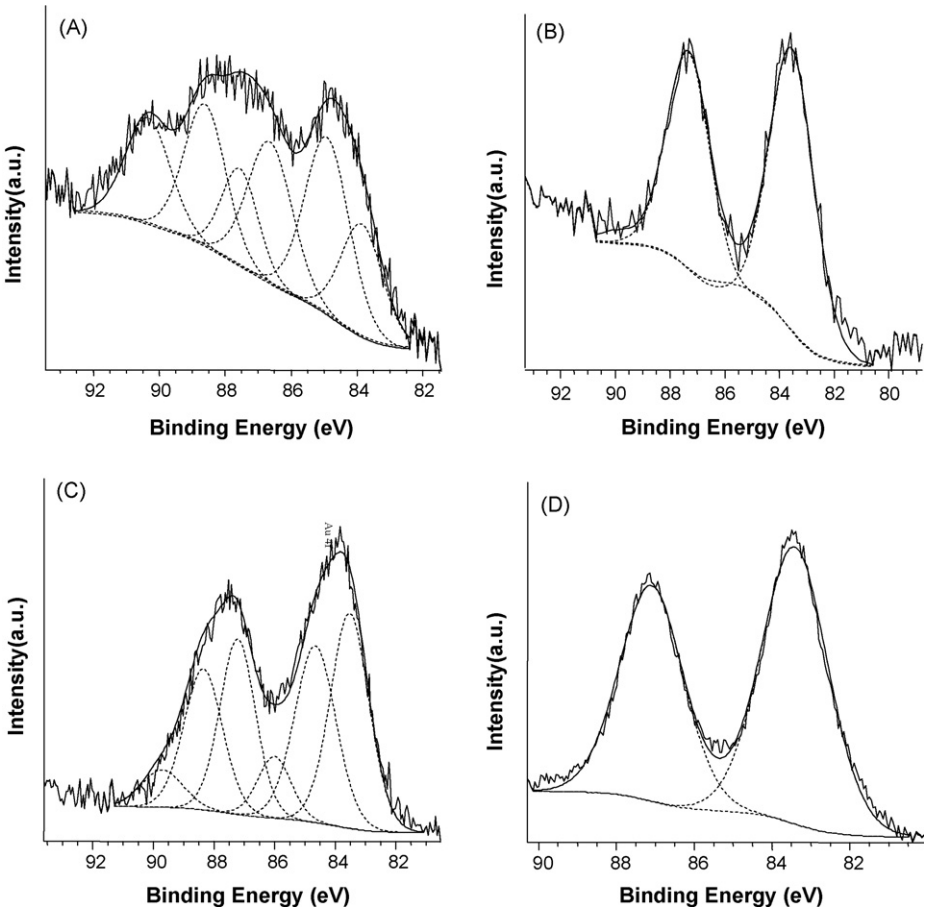

Fig. 4. XPS spectra of (A) 1% Au/CeO_2 activated under O_2/He at 500 °C, (B) 1% Au/CeO_2 activated under H_2 at 300 °C, (C) 4% Au/CeO_2 activated under O_2/He at 500 °C and (D) 4% Au/CeO_2 activated under H_2 at 300 °C.

reducibility of ceria surface oxygen [52–54]. The small size of the ceria nanoparticles (around 5 nm, estimated by XRD) of the high surface ceria employed in this study may also participate to the observed high activity as previously reported for CO oxidation [55]. Thus, the high activity of the Au/CeO_2 system in the propene oxidation reaction should be regarded as a synergetic interplay between gold and ceria.

After calcination, gold on ceria (1 wt% Au) is more active than ceria alone (Fig. 1) although gold is still in the oxidation state +III. It indicates that the presence of gold(III) may modify and enhance the catalytic properties of ceria. Indeed, Deng et al. [40] reported that addition of gold has a major effect in suppressing the crystal growth of ceria, and Leppelt et al. [56] showed that the Ce^{3+} concentration in ceria increased from 10 to 22% during reduction treatment in hydrogen at 200 °C as the gold loading increased from 0.8 to 12.6 wt%. It is worth to note that the catalyst colour turned from yellow to dark brown during propene oxidation, which may indicate that the gold oxidation state changes during the reaction. Moreover, as the low loaded Au/CeO_2 catalysts activated under H_2 are more active than after calcination (Fig. 3), metallic gold seems to be the most active species.

To investigate the possible reduction of gold on ceria (1 wt% Au) during propene oxidation, the following experiment was performed. The 1 wt% Au/CeO_2 sample *in situ* calcined at 500 °C was submitted to propene oxidation from RT to 500 °C. After measurement of propene conversion at the various increasing temperatures, the catalyst was cooled down to RT under O_2 in He, and the activity in CO oxidation was measured at RT in order to evaluate the oxidation state of gold (for more details about the experiment, see Section 2.3). The results of propene conversion and CO activity versus temperature are displayed in Fig. 5. Initially, the catalyst is not active in CO oxidation at room temperature. While the catalyst starts to show activity in propene oxidation, activity in CO oxidation is also detected, indicating that gold starts reducing. Between 150 and 175 °C, the curve of propene conversion exhibits an inflexion point and CO activity drastically increases. At 200 °C, 100% conversion of propene is reached and CO activity is maximum. When temperature is higher than 200 °C, CO activity decreases. This is especially drastic between 300 and 500 °C. This experiment indicates that the oxidation state of gold in the calcined 1 wt% Au/CeO_2 sample changes during propene oxidation from Au^{III} to Au^0 between RT and 200 °C, then the decrease of activity in CO oxidation between 300 and 500 °C indicates either that gold particles sinter or that part of the gold reoxidises. However, XRD analyses did not reveal the presence of diffraction lines of metallic gold after propene oxidation on Au/CeO_2 up to 500 °C, which does not support the assumption of a sintering of the gold particles.

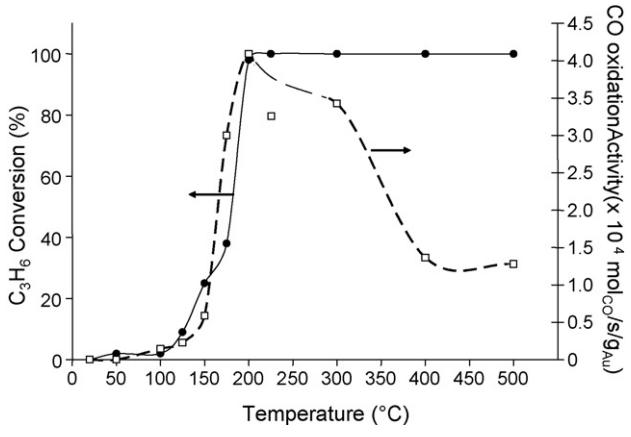

Fig. 5. Propene conversion and subsequent CO oxidation activity at RT versus propene oxidation temperature for 1% Au/CeO_2 activated under O_2/He at 500 °C.

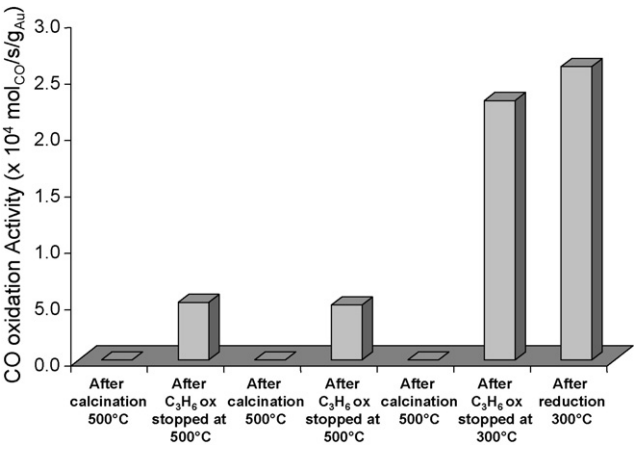

Fig. 6. CO oxidation activity at RT for a 1% Au/CeO_2 catalyst after activation under O_2/He at 500 °C and after several cycles of activation under O_2/He at 500 °C or H_2 at 300 °C and propene oxidation up to 500 or 300 °C.

In order to go further in the interpretations, the activity in CO oxidation at room temperature was evaluated after cycles of activation/propene oxidation over the 1 wt% Au/CeO_2 sample (Fig. 6). After activation under O_2/He at 500 °C, no activity in CO oxidation at RT was detected, as previously observed. This can be correlated to the absence of metallic gold species in the calcined sample (Table 1). After propene oxidation carried out up to 500 °C, some activity in CO oxidation is detected, indicating that metallic gold was formed during the reaction. Another calcination under O_2/He at 500 °C resulted in an inactive sample, then, the previous activity is recovered after a new cycle of propene oxidation up to 500 °C. Interestingly, higher activity is observed after a new calcination under O_2/He at 500 °C followed by propene oxidation reaction interrupted at 300 °C. Subsequent activation under H_2 at 300 °C led to a slight further increase in activity in CO oxidation. These experiments confirm that reduction of gold occurred during propene oxidation. They show in addition that this reduction is reversible when the sample is re-activated under O_2/He at 500 °C. The catalyst behaviour during the series of activation/propene oxidation experiments does not support the hypothesis of a sintering of the gold particles during propene oxidation between 300 and 500 °C. Indeed, this hypothesis is not consistent with the fact that higher activity in CO oxidation can be further obtained when propene oxidation was interrupted at 300 °C or when the sample was activated under H_2. The activity in CO oxidation at RT depends on the final temperature of propene oxidation, which can be related to variation in the extent of the reduction, more metallic gold being formed when reaction is performed up to 300 °C instead of 500 °C. After propene oxidation at 300 °C, gold is almost fully reduced as indicated by the fact that activity in CO oxidation is almost the same as that of the sample activated under H_2 at 300 °C.

To complement these results, another experiment was performed in the DRIFTS cell and the oxidation state of gold was probed *via* the adsorption of CO for 10 min at room temperature after that propene oxidation was carried out in the cell by stepwise increase of the temperature (Fig. 7A). After calcination under O_2/He at 500 °C, the adsorption of CO revealed the presence of a main band centred at 2158 cm^{-1} (Fig. 7A, spectrum (a)). According to literature, this band could be assigned to the adsorption of CO on cations (Au^+ or support cations) [57–63]. The fact that a part of the band persists when the cell is evacuated under He (not shown) favours the assumption that Au^+ species is present on the Au/CeO_2 sample after calcination since CO adsorption on Ce^{4+} or Ce^{3+} is

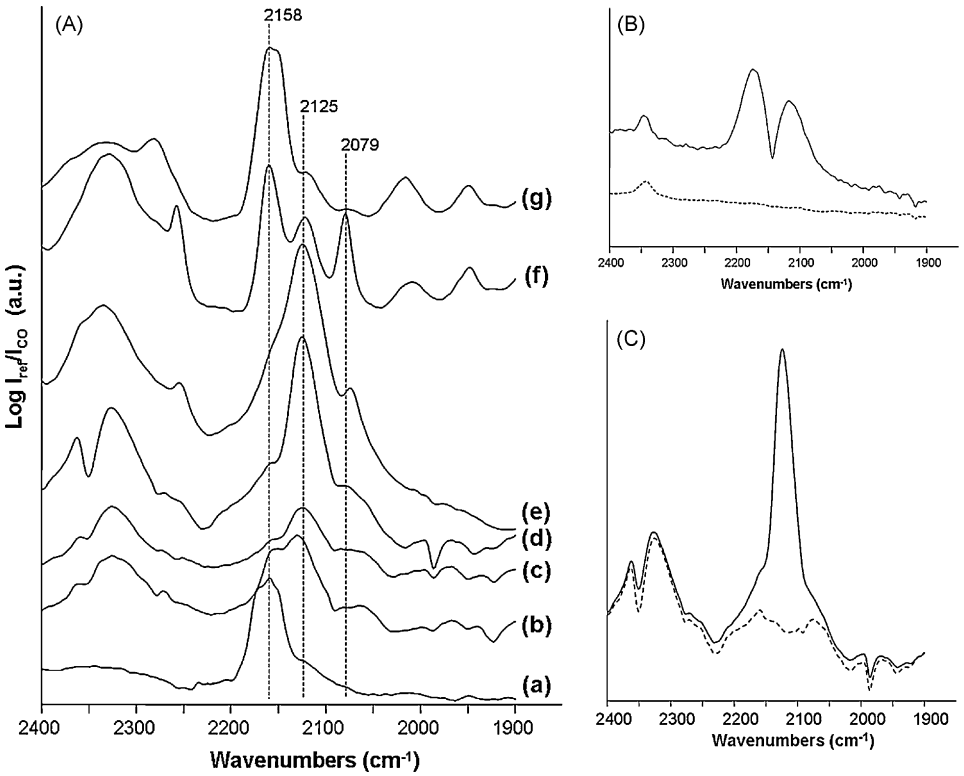

Fig. 7. DRIFT spectra of CO adsorption (1% CO in He) at RT for (A) 1% Au/CeO_2 after calcination at 500 °C (a) and after C_3H_6 oxidation at 100 °C (b), 150 °C (c), 200 °C (d), 300 °C (e), 400 °C (f), 500 °C (g). (B) CeO_2 after calcination at 500 °C under CO/He (solid line) and after evacuation under He for 2 min (dotted line). (C) Spectrum (Ad) under CO/He (solid line) and after evacuation under He for 2 min (dotted line).

considered as weak and therefore CO adsorbed on cerium cations is easily removed upon evacuation. Moreover, when CO adsorption was performed at room temperature on the pure CeO_2 support calcined under O_2/He at 500 °C, only CO in gas phase was visible with no CO adsorption on the support and no contribution remaining after evacuation under He (Fig. 7B). We have showed previously by XAFS that Au^{3+} species is the main species after calcination. The CO adsorption on Au^{3+} species is rarely reported in the literature. One explanation is that Au^{3+} ions are very easily reduced by CO at RT [64–67]. Such a reduction can result in the formation of the Au^{+} species that can also be reduced to Au^{0} under further contact with CO atmosphere [64]. Indeed, a weak shoulder to the main band can be observed around 2125 cm^{-1}. Such a frequency is correlated in the literature to the adsorption of CO on low coordinated metallic Au^{0} sites [67–71] or on slightly positively charged $Au^{\delta+}$ sites [46,74]. The presence of such sites, which can be qualified as reduced gold sites, would indicate the existence of small amount of reduced gold species in the catalyst after calcination. In summary, the CO adsorption on the calcined Au/CeO_2 sample indicates that gold is mainly under an oxidised form, which is in agreement with the previous characterisation by XAFS and XPS and with the lack of activity in CO oxidation.

When CO adsorption is performed at RT after propene oxidation (Fig. 7A) at 100 °C (spectrum (b)), 150 °C (c) and 200 °C (d), the band at low wavenumbers (2120–2130 cm^{-1}) starts to increase whereas the one at high frequency (2150–2160 cm^{-1}) progressively decreases. This trend indicates that the oxidised gold species are readily reduced during the propene oxidation reaction and that the extent of the reduction increases when the temperature of propene oxidation is raised from 100 to 200 °C. The average frequency of the band assigned to CO adsorbed on reduced gold species (2125 cm^{-1}) is also close to the one that is ascribed in the literature to the forbidden electronic transition of Ce^{3+} ions [72,73]. According to the same papers [72,73], this electronic transition resulting from the reduction of the ceria by CO should persist during evacuation under He. Fig. 7C shows that the band at 2125 cm^{-1} almost disappears under He, confirming that this band is related to the adsorption of CO on metallic gold sites. A very recent study on the interaction of gold with cerium oxide supports showed that ceria nanoparticles stabilise gold nanoparticles in strong interaction with the support, leading to positively charged gold species, characterised by a CO vibration frequency at around 2125 cm^{-1}, above the typical wavenumber of CO adsorbed on purely metallic gold (2100–2110 cm^{-1}) [46]. Thus, it may be inferred that gold reduction during the propene oxidation reaction results in the formation of small gold clusters in strong interaction with the ceria. Other bands at low wavenumber (2080, 2015 and 1950 cm^{-1}) grow up when the temperature of propene oxidation increases up to 400 °C (Fig. 7A, spectra (e) and (f)). Because of their low wavenumbers compared to metallic gold, they could be assigned to electron-rich gold sites, resulting from a charge transfer from the partially reduced CeO_2 support to the gold nanoparticles [60,71,74,75] or to Au–Ce alloy clusters [76]. When the propene oxidation temperature is above 300 °C (Fig. 7A, spectra (e–g)), a progressive decrease of the intensity of the band at 2125 cm^{-1} is observed, in parallel with the increase of the band at 2158 cm^{-1}, and the band at 2080 cm^{-1} almost disappear at 500 °C. Clearly, reoxidation of some gold atoms of the reduced gold nanoparticles occurs during propene oxidation at high temperature, in agreement with the activity in CO oxidation (Figs. 5 and 6), which decreases when the temperature of propene oxidation is above 300 °C.

Reoxidation of gold on ceria has already been reported by several groups. Tibiletti et al. [77] reported a reoxidation of 15% of metallic gold when a 2 wt% Au/CeO_2–ZrO_2 sample reduced during Water Gas Shift reaction, was exposed to air at 150 °C. The reoxidation is attributed to the gold atoms of metal particles in contact with the support. Karpenko et al. also observed gold partial

reoxidation by XPS after Au/CeO_2 (2.8 wt%) reduction during WGS reaction after exposure to H_2O/N_2 (19% Au^{III}) or to O_2/N_2 (28% Au^{III}) at 400 °C [78]. In a very recent paper, Deng et al. also reported that a 0.5 wt% Au/CeO_2 reduced during WGS reaction at 200 °C (53% Au^0) was fully reoxidised in oxygen at 400 °C [33].

4. Conclusion

This work shows that, among the studied supports, ceria is the most appropriate support for the total oxidation of propene using gold catalysts. Characterisations by XPS and using CO oxidation as a probe reaction reveal the influence of both the activation conditions and the gold loading on the oxidation state of gold supported on high specific surface ceria. Regarding the propene oxidation reaction, propene can be totally converted into CO_2 at temperature as low as 200 °C on Au/CeO_2. Activation under H_2 is beneficial to the activity, indicating that metallic gold is required for the reaction, which is supported by the observation that the initial Au^{III} species in an Au/CeO_2 calcined sample are reduced during the reaction. Reoxidation of gold was also observed between 300 and 500 °C when 100% conversion of propene was achieved.

Acknowledgement

The authors acknowledge the ANR (Agence Nationale pour la Recherche), which sponsored this work (ANR- BLANC07-2 183612).

References

[1] S. Minicò, S. Scirè, C. Crisafulli, S. Galvagno, Appl. Catal. B Environ. 34 (2001) 277–285.
[2] S. Minicò, S. Scirè, C. Crisafulli, R. Maggiore, S. Galvagno, Appl. Catal. B Environ. 28 (2000) 245–251.
[3] S. Scirè, S. Minicò, C. Crisafulli, S. Galvagno, Catal. Commun. 2 (2001) 229–232.
[4] M.A. Centeno, M. Paulis, M. Montes, J.A. Odriozola, Appl. Catal. A 234 (2002) 65–78.
[5] A.C. Gluhoi, N. Bogdanchikova, B.E. Nieuwenhuys, J. Catal. 229 (2005) 154–162.
[6] M.L. Jia, H.F. Bai Zhaorigetu, Y.N. Shen, Y.F. Li, J. Rare Earths 26 (2008) 528–531.
[7] B. Solsona, T. Garcia, R. Murillo, A.M. Mastral, E.N. Ndifor, C.E. Hetrick, M.D. Amiridis, S.H. Taylor, Top. Catal. 52 (2009) 492–500.
[8] S. Scire, S. Minico, C. Crisafulli, C. Satriano, A. Pistone, Appl. Catal. B Environ. 40 (2003) 43–49.
[9] D. Andreeva, P. Petrova, J.W. Sobczak, L. Ilieva, M. Abrashev, Appl. Catal. B Environ. 67 (2006) 237–245.
[10] M. Haruta, Chem. Record 3 (2003) 75–87.
[11] M. Haruta, Catal. Today 36 (1997) 153–166.
[12] S. Ivanova, C. Petit, W. Pitchon, Colloquium on Environment, Materials, Energy, Elsevier Science BV, Ouargla, Algeria, 2004, pp. 182–186.
[13] V.R. Choudhary, V.P. Patil, P. Jana, B.S. Uphade, Appl. Catal. A Gen. 350 (2008) 186–190.
[14] H.G. Ahn, B.M. Choi, D.J. Lee, International Conference on Nanoscience and Nanotechnology, Amer Scientific Publishers, Gwangju, South Korea, 2005 , pp. 3599–3603.
[15] K. Blick, T.D. Mitrelias, J.S.J. Hargreaves, G.J. Hutchings, R.W. Joyner, C.J. Kiely, F.E. Wagner, Catal. Lett. 50 (1998) 211–218.
[16] R.D. Waters, J.J. Weimer, J.E. Smith, Catal. Lett. 30 (1995) 181–188.
[17] S.J. Miao, Y.Q. Deng, Appl. Catal. B Environ. 31 (2001) L1–L4.
[18] M. Haruta, Now Future 7 (1992) 13.
[19] L. Delannoy, N. Weiher, N. Tsapatsaris, A.M. Beesley, L. Nchari, S.L.M. Schroeder, C. Louis, Top. Catal. 44 (2007) 263–273.
[20] R. Zanella, S. Giorgio, C.R. Henry, C. Louis, J. Phys. Chem. B 106 (2002) 7634–7642.
[21] R. Zanella, L. Delannoy, C. Louis, Appl. Catal. A 291 (2005) 62–72.
[22] R. Zanella, C. Louis, Catal. Today 107–108 (2005) 768–777.
[23] A. Karpenko, R. Leppelt, V. Plzak, J. Cai, A. Chuvilin, B. Schumacher, U. Kaiser, R.J. Behm, Top. Catal. 44 (2007) 183–198.
[24] T.L. Barr, S. Seal, L.M. Chen, C.C. Kao, Thin Solid Films 253 (1994) 277–284.
[25] M. Romeo, K. Bak, J. Elfallah, F. Lenormand, L. Hilaire, Surf. Interface Anal. 20 (1993) 508–512.
[26] J.H. Scofield, J. Electron Spectrosc. Relat. Phenom 8 (1976) 129–137.
[27] P. Concepcion, S. Carrettin, A. Corma, Appl. Catal. A Gen. 307 (2006) 42–45.
[28] S. Carrettin, A. Corma, M. Iglesias, F. Sanchez, Appl. Catal. A 291 (2005) 247–252.
[29] F. Vindigni, M. Manzoli, A. Chiorino, T. Tabakova, F. Boccuzzi, J. Phys. Chem. B 110 (2006) 23329–23336.
[30] A. Karpenko, R. Leppelt, V. Plzak, R.J. Behm, J. Catal. 252 (2007) 231–242.
[31] A. Karpenko, Y. Denkwitz, V. Plzak, J. Cai, R. Leppelt, B. Schumacher, R.J. Behm, Catal. Lett. 116 (2007) 105–115.
[32] Q. Fu, H. Saltsburg, M. Flytzani-Stephanopoulos, Science 301 (2003) 935–938.
[33] W. Deng, A.I. Frenkel, R. Si, M. Flytzani-Stephanopoulos, J. Phys. Chem. C 112 (2008) 12834–12840.
[34] R. Zanella, S. Giorgio, C.-H. Shin, C.R. Henry, C. Louis, J. Catal. 222 (2004) 357–367.
[35] J.T. Miller, A.J. Kropf, Y. Zha, J.R. Regalbuto, L. Delannoy, C. Louis, E. Bus, J.A. van Bokhoven, J. Catal. 240 (2006) 222–234.
[36] A. Hugon, L. Delannoy, C. Louis, Gold Bull. 41 (2008) 127–138.
[37] R. Holm, S. Storp, Appl. Phys. 9 (1976) 217–222.
[38] W. McLean, C.A. Colmenares, R.L. Smith, G.A. Somorjai, J. Phys. Chem. 87 (1983) 788–793.
[39] H. Kitagawa, N. Kojima, T. Nakajima, J. Chem. Soc. Dalton Trans. (1991) 3121–3125.
[40] W. Deng, J.D. Jesus, H. Saltsburg, M. Flytzani-Stephanopoulos, Appl. Catal. A 291 (2005) 126–135.
[41] C.J. Weststrate, A. Resta, R. Westerstrom, E. Lundgren, A. Mikkelsen, J.N. Andersen, J. Phys. Chem. C 112 (2008) 6900–6906.
[42] A. McNeillie, D.H. Brown, W.E. Smith, M. Gibson, L. Watson, J. Chem. Soc. Dalton Trans. (1980) 767–770.
[43] Q. Fu, W. Deng, H. Saltsburg, M. Flytzani-Stephanopoulos, Appl. Catal. B Environ. 56 (2005) 57–68.
[44] D. Andreeva, I. Ivanov, L. Ilieva, J.W. Sobczak, G. Avdeev, T. Tabakova, Appl. Catal. A Gen. 333 (2007) 153–160.
[45] D. Andreeva, I. Ivanov, L. Ilieva, M.V. Abrashev, R. Zanella, J.W. Sobczak, W. Lisowski, M. Kantcheva, G. Avdeev, K. Petrov, Appl. Catal. A Gen. 357 (2009) 159–169.
[46] M. Baron, O. Bondarchuk, D. Stacchiola, S. Shaikhutdinov, H.J. Freund, J. Phys. Chem. C 113 (2009) 6042–6049.
[47] M. Haruta, S. Tsubota, T. Kobayashi, H. Kageyama, M.J. Genet, B. Delmon, J. Catal. 144 (1993) 175–192.
[48] E.A. Willneff, S. Braun, D. Rosenthal, H. Bluhm, M. Hävecker, E. Kleimenov, A. Knop-Gericke, R. Schlögl, S.L.M. Schroeder, J. Am. Chem. Soc. 128 (2006) 12052–12053.
[49] A. Trovarelli, Catalysis by Ceria and Related Materials, vol. 891, Imperial College Press, London, 2002.
[50] S. Scirè, S. Minicò, C. Crisafulli, C. Satriano, S. Galvagno, Appl. Catal. B Environ. 40 (2003) 43–49.
[51] E. Finocchio, G. Busca, V. Lerenzelli, V.S. Escribano, J. Chem. Soc. Faraday Trans. 92 (1996) 1587–1593.
[52] Q. Fu, A. Weber, M. Flytzani-Stephanopoulos, Catal. Lett. 77 (2001) 87–95.
[53] A.M. Venezia, G. Pantaleo, A. Longo, G.D. Carlo, M.P. Casaletto, F.L. Liotta, G. Deganello, J. Phys. Chem. B 109 (2005) 2821–2827.
[54] S.-Y. Lai, Y. Qiu, S. Wang, J. Catal. 237 (2006) 303–313.
[55] S. Carrettin, P. Concepcion, A. Corma, J.M.L. Nieto, V.F. Puntes, Angew. Chem. 43 (2004) 2538–2540.
[56] R. Leppelt, B. Schumacher, V. Plzak, M. Kinne, R.J. Behm, J. Catal. 244 (2006) 137–152.
[57] F. Boccuzzi, A. Chiorino, S. Tsubota, M. Haruta, J. Phys. Chem. 100 (1996) 3625–3631.
[58] S. Minicò, S. Scirè, C. Crisafulli, A.M. Visco, S. Galvagno, Catal. Lett. 47 (1997) 273–276.
[59] F. Boccuzzi, A. Chiorino, M. Manzoli, Surf. Sci. 454–456 (2000) 942–946.
[60] T. Tabakova, F. Boccuzzi, M. Manzoli, D. Andreeva, Appl. Catal. A 252 (2003) 385–397.
[61] M. Manzoli, F. Boccuzzi, A. Chiorino, F. Vindigni, W. Deng, M. Flytzani-Stephanopoulos, J. Catal. 245 (2007) 306–313.
[62] C. Binet, M. Daturi, J.C. Lavalley, Catal. Today 50 (1999) 207–225.
[63] C. Li, Y. Sakata, T. Arai, K. Domen, K. Maruya, T. Onishi, J. Chem. Soc. Faraday Trans. 85 (1989) 929–943.
[64] T. Venkov, K. Fajerwerg, L. Delannoy, K. Klimev, K. Hadjiivanov, C. Louis, Appl. Catal. A 301 (2006) 106–114.
[65] M.Y. Mihaylov, J.C. Fierro-Gonzalez, H. Knozinger, B.C. Gates, K.I. Hadjiivanov, J. Phys. Chem. B 110 (2006) 7695–7701.
[66] H. Klimev, K. Fajerwerg, K. Chakarova, L. Delannoy, C. Louis, K. Hadjiivanov, J. Mater. Sci. 42 (2007) 3299–3306.
[67] M. Mihaylov, H. Knozinger, K. Hadjiivanov, B.C. Gates, Chem. Ing. Technol. 79 (2007) 795–806.
[68] M.A. Bollinger, M.A. Vannice, Appl. Catal. B Environ. 8 (1996) 417–443.
[69] K. Hadjiivanov, G. Vayssilov, Adv. Catal. 47 (2002) 347.
[70] G.C. Bond, D.T. Thompson, Catal. Rev. Sci. Eng. 41 (1999) 319–388.
[71] F. Boccuzzi, A. Chiorino, M. Manzoli, Mater. Sci. Eng. C Biomimetic Supramol. Syst. 15 (2001) 215–217.
[72] H. Daly, J. Ni, D. Thompsett, F.C. Meunier, J. Catal. 254 (2008) 238–243.
[73] C. Binet, A. Badri, J.C. Lavalley, J. Phys. Chem. 98 (1994) 6392–6398.
[74] R. Meyer, C. Lemire, S.K. Shaikhutdinov, H.J. Freund, Gold. Bull. 37 (2004) 72–124.
[75] L. Delannoy, N.E. Hassan, A. Musi, N. Nguyen Le To, J.-M. Krafft, C. Louis, J. Phys. Chem. B 110 (2006) 22471–22478.
[76] G. Avgouropoulos, M. Manzoli, F. Boccuzzi, T. Tabakova, J. Papavasiliou, T. Ioannides, V. Idakiev, J. Catal. 256 (2008) 237–247.
[77] D. Tibiletti, A. Amieiro-Fonseca, R. Burch, Y. Chen, J.M. Fisher, A. Goguet, C. Hardacre, P. Hu, A. Thompsett, J. Phys. Chem. B 109 (2005) 22553–22559.
[78] A. Karpenko, R. Leppelt, J. Cai, V. Plzak, A. Chuvilin, U. Kaiser, R.J. Behm, J. Catal. 250 (2007) 139–150.